

Measurement of Two Phase Flows in Geothermal Pipelines Using Load-Cells: Field Trial Results

John R. SISLER^{1*}, Sadiq J. ZARROUK¹, Alex URGEL², Yoong Wei LIM², Richard ADAMS³
and Steven MARTIN⁴

¹ Department of Engineering Science, University of Auckland, Private Bag: 92019, Auckland 1142, New Zealand.

² Contact Energy Ltd., Private Bag 2001, Taupo 3362, New Zealand.

³ MB Century Ltd, P.O. Box: 341, Taupo, 3351, New Zealand.

⁴ Department of Physics, University of California, Santa Cruz, 95064, USA*jsisler@cruzio.com

Keywords: Geothermal flow measurement, well discharge testing, two-phase, horizontal discharge, enthalpy, dryness fraction, orifice plate, mass flow rate, tracer flow test.

ABSTRACT

A method for the measurement of two phase flow has been tested, with the ability to provide continual monitoring of two-phase flow in geothermal or other pipelines. The sensor uses strain gage measurement on pipe supports to measure flow characteristics in a large volume of piping from one pipe support to another. Horizontal discharge well output tests were performed on wells at Wairakei geothermal field, New Zealand, with the sensor included during the tests for performance comparison and calibration to the standard output test. The sensor is able to accurately track changes in the flow, with the advantage of simple construction, no direct contact required with internal pipe content, no restriction to the flow, and easy setup. The sensor can track changes in the percent of steam to water in the pipe, for the calculation of enthalpy from the well in real time. The method has the potential to complement (improve) the accuracy of existing two-phase orifice plates, or as a stand-alone method for the measurement of total mass flow rate and enthalpy in geothermal pipelines and wells. Accurate tracking of changes to dryness fraction were observed, as well as detection of other phenomenon. Results of field trials and calibration methods are presented.

1. INTRODUCTION

1.1 Geothermal steam field management

Development of electrical power from geothermal sources requires continual monitoring and planning to maintain or improve the energy output from such facilities. In New Zealand, continuous fluid flow measurement and monitoring is also a primary condition for resource consent and compliance. Maximizing the production from all wells and sources is a balancing act of knowing how the available wells will perform, when to plan for additional wells, and how to determine the most effective time to perform maintenance or other required operations. The more that can be known about well output performance, the better such plans can be made. Two important parameters to determine from each well are flow rate and enthalpy, and how these may change over time either by themselves or by interaction with other wells in operation. Various techniques have been devised to determine these two parameters, with most methods complicated by the fact that well production is often two-phase. The techniques are not suited to continual measurement on a minute or hourly basis. The common practice is to perform such tests only quarterly or longer, due to expense of testing or the requirement that the test be performed while the well is out of service. Changes occurring in the wells, or interaction between wells, may be missed with such long timespans between test results. The sensor method discussed here can provide data through these long timespans, providing results minute by minute, and may help improve the activity of tuning the steam field system for maximum performance and efficiency.

1.2 The sensor method

Piping in geothermal fields is often held above ground on pipe supports. Supports in some locations are allowed to slide to accommodate thermal expansion/contraction. This aspect of steam field design is used to allow for a measurement of pipe and fluid weight by monitoring the overall weight seen at one or more sliding pipe supports. One or two sensors are attached to one or two pipe supports of a well output, and calibrated to the specifics of the pipe geometry. Data can be taken continuously. Results of field trials taken during static flow and horizontally discharged well output tests are included and discussed.

2. MEASUREMENT WITH LOADCELLS

2.1 Introduction

The sensor method determines the contents of the pipe by weighing the overall structure. Many factors may affect the weight reading detected; such as pipe stresses, support from other locations, and properties of the water itself. Computer models of piping structures were created using Solidworks™ Simulation to allow study of various potential additional stresses, with specific models of pipe geometries similar to those expected at the field trial locations studied in detail.

2.2 Pipe geometries

Steel piping used in steam fields is a strong element, able to support itself between pipe supports. A simple static load model (without pipe stress being considered) can help determine the expected weight seen at a center support in a pipe supported at each end, such as that shown in Figure 1 below.

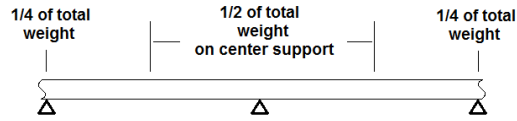


Figure 1: Simple static model

In this simple model, without taking pipe strength into account, the weight measured at the center would be expected to be one half of the total weight of the structure.

In a circumstance where the center support is offset a small amount from center, this simplistic model of weight would still be the same, as shown in the Figure 2.

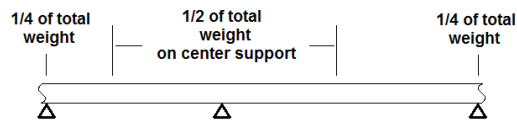


Figure 2: Simple static model with minor offset of center support.

Actual structures would be expected to have pipe stresses that may affect the weight seen on a centralized support. If for example the pipe is fixed to a rigid support at one or both ends, this may affect the weight seen on a central support. A rigid support near the sensor location may allow the pipe itself to hold much of the weight of the unsupported span, similar to a cantilever, whereas a sliding support will not. These potential additional stresses were studied with Solidworks™ Simulation to determine the extent of support that may be expected from a fixed location as well as effects of offset center supports. The simulation model includes necessary parameters such as steel type, pipe diameter, wall thickness, distance between supports, support type (whether fixed or sliding), extra weight of insulation, weight of insulation protective covers, and material properties of all structural elements as well as for the water in the pipe. Material properties were adjusted for performance in the expected temperature range of operation.

Results show that pipe stresses of these kinds do not contribute greatly to measurement inaccuracy of the small changes in weight expected to be seen from variance in the material flowing in the pipe. The simulations show that the long distances between pipe supports allow for an accurate measurement of varying weight at the center of the span without significant effects from fixed supports or other pipe stresses. In the simulations, all effects from such stresses do not contribute more than the equivalent of a 1% change in water content in the piping, and such effects are able to be predicted if needed. The simulations did show that pipe pressure may have an effect on pipe stresses, in pipes of larger diameter. These results suggest that a simple calculation as shown in Figure 1 is sufficient for determination of the expected weight in the center of a span. From this calculation, the necessary load cell maximum capacity was determined, as well as the expected weight of a 1% change in water content. The weight of a 1% change in water content in the pipes for various field trial locations was determined from the simulation studies, summarized below:

Location 1 and 3: 1% water delta = 7.78 kg Location 2: 1% water delta = 5.94 kg Location 4: 1% water delta = 18.1 kg

2.3 Field installation

With the expected weights determined, suitable mounts for the sensors were designed and fabricated to match the various possible sizes and shapes of pipe supports, while also meeting the necessary safety requirements. The design allows the weight of the pipe to be on the load cell while still allowing the pipe support itself to be the main element responsible for pipe alignment, as shown in Figures 3 and 4.



Figure 3: Load cell on load cell stand



Figure 4: Load cell detail.

Once in place the load cells did not experience any movement, and a simple strap held the load cell and stand firmly against the pipe supports is sufficient for the test. A laptop computer was used for data acquisition and the data was logged and reviewed after completion of tests. Data points were taken approximately 35 times per second (35 Hz).

3. HORIZONTAL DISCHARGE FIELD TRIAL LOCATIONS

3.1 Initial results

The sensors were installed to pipe supports on wells that were undergoing standard horizontal discharge well outputs tests. Four separate locations were used. The four locations have different pipe geometries as explained below.

3.2 Location 1: wk260

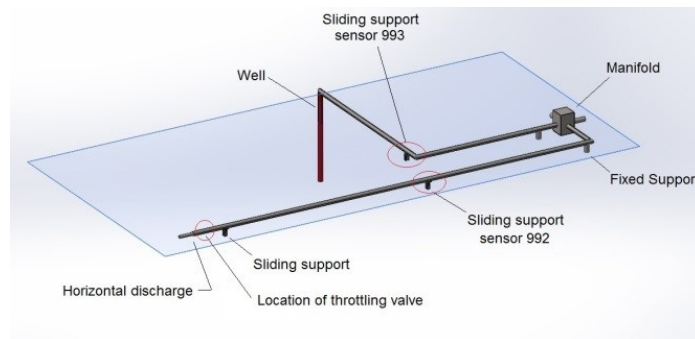


Figure 5: Location 1 (wk260) field piping.

Two sensors were mounted as shown in Figures 3-4. The well output was diverted at the manifold into the horizontal discharge line for the well output test. Lip pressure data was taken at the horizontal discharge, and wellhead pressure controlled at the valve near the horizontal discharge. The well was allowed to run full then throttled in two steps, with sufficient time to allow for stable flow between steps. This created three different flow regimes, and well output data for the horizontal discharge test was taken for each regime. The sensor itself took data continuously, resulting in the dataset shown in Figure 6.

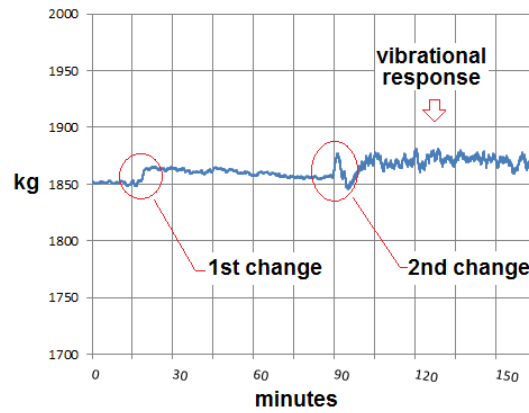


Figure 6: Location 1 (wk260) initial results. Total measured weight vs time.

The result shows an increase in weight throughout each change. After the second valve change the well piping was showing signs of vibration and was defined as ‘choked’, or close to the maximum discharge pressure (MDP). The Sensor registered an increase in vibration during this time, but an overall average increase in weight is still visible in the data.

Responses such as this were typical from all four test locations. Data sets show details of each valve change, showing the sensor’s ability to track changes in real time.

3.3 Location 2: wk253

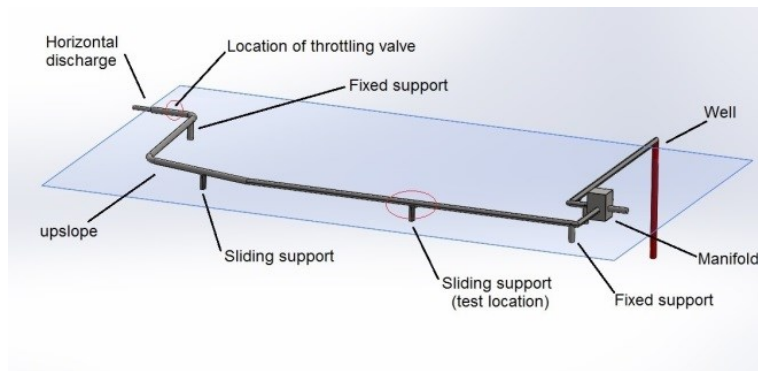


Figure 7: Location 2 (wk253) field piping

Location 2 has different pipe geometry, with piping that is fixed at two points. One fixed support is near the manifold and the other is located around a 90 degree bend near the horizontal discharge. Also, the piping actually measured by the sensor is not level, but has a rise in elevation that begins between the sliding supports, as seen in Figure 7. Like location 1 the well was allowed to run full, then throttled in two steps with a short time between steps to allow the flow to stabilize. This created three different flow regimes. Results of the raw data-set are shown in Figure 8.

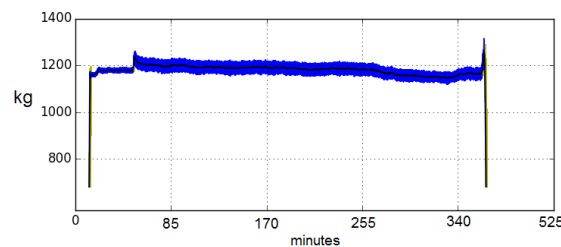


Figure 8: Location 2 (wk253) raw dataset

The first and second valve adjustments can be seen occurring before 85 minutes. No additional valve adjustments were made after this time. At approximately 255 minutes a decrease in measured weight occurred. These changes are shown in details in Figures 9 and 10.

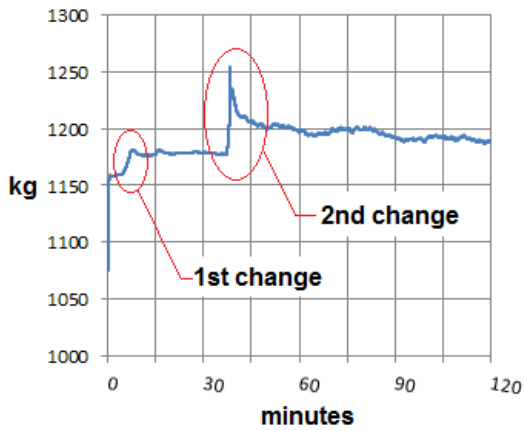


Figure 9: Location 2 (wk253) valve changes

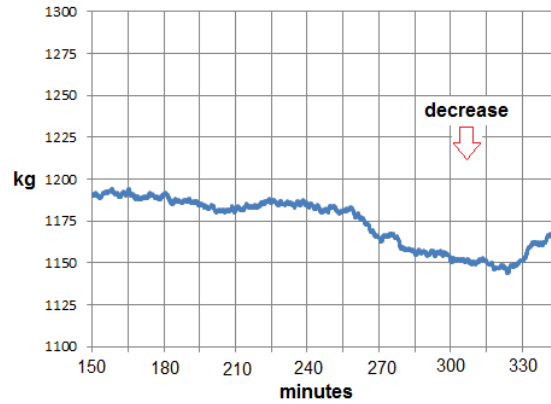


Figure 10: Location 2 (wk253) afternoon decrease

The decrease in weight seen in figure 10 apparently occurred on its own, without any planned change to WHP, and would indicate that the dryness fraction of the well flow had increased. The well output may have changed, and contained more steam and less water.

3.4 Location 3: wk258

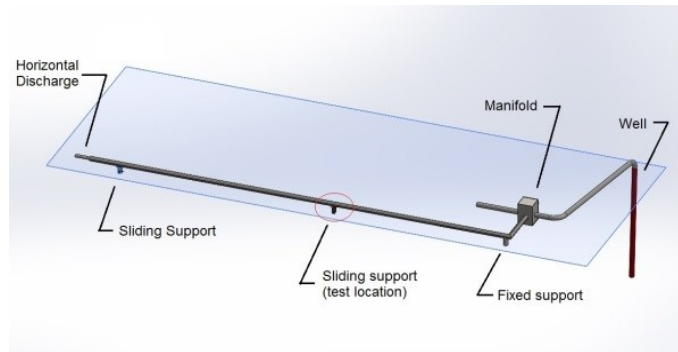


Figure 11: Location 3 (wk258) field piping

Location 3 (wk258) uses the same piping as location 1. The sensor was placed on the same pipe support as in location 1, though the flow to the horizontal discharge is from a different well. The well was throttled in one step, creating only two different flow regimes. To determine effects of pipe stress, a weight of known amount was set on the pipe for a few minutes, after the valve change. This ‘standard weight’ allowed for a determination of test accuracy, and whether or not pipe stress or other phenomenon were effecting the weight being measured. The addition of the standard weight can be seen in the dataset shown in Figure 12.

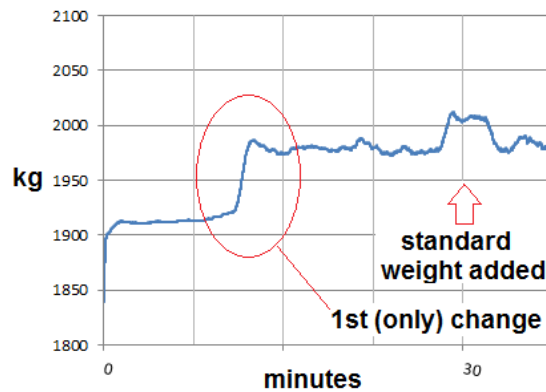


Figure 12: Location 3 (wk285) valve change and standard weight.

The standard weight added to the pipe weighs of 30.6kg. A review of the data shows that the increase in weight seen when the standard weight was added to the pipe was 30.8 kg. This would indicate that pipe stresses have little effect on the overall weight measurement obtained from the sensor.

3.5 Location 4: wk222

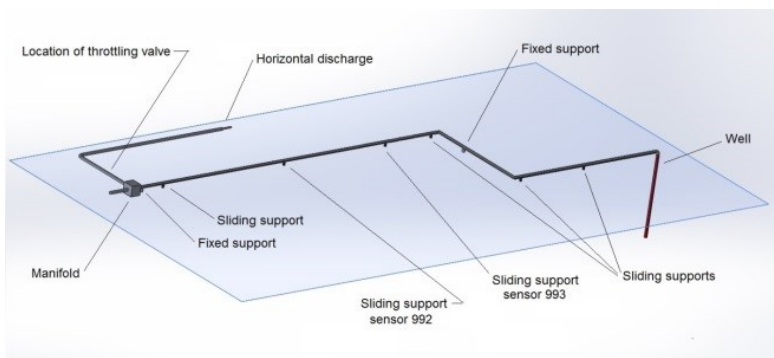


Figure 12: Location 4 (wk222) field piping.

Test location 4 (wk222) is considerably different from test locations 1 through 3. The sensors were placed on two pipe supports on the main line from the well, not on a line to the horizontal discharge. The well output was diverted to the horizontal discharge line at the manifold. Lip pressure data was taken at the horizontal discharge, and wellhead pressure controlled at a valve in the discharge line. The well was allowed to run full then throttled in two steps, with sufficient time between steps to allow the flow to stabilize. This created three different flow regimes. The same standard weight used in location 3 was added to the pipe for a few minutes at location 4 (wk222) to help determine if pipe stresses may be holding the pipe up more than expected. A small change in weight was found, the equivalent of .12% of water weight in the pipe. Simulation studies for location 4 (wk222) suggest that such an effect on weight may be due to the pressure effect becoming a factor in the larger diameter pipe at this location.

4. COMPARISON OF SENSOR DATA TO HORIZONTAL DISCHARGE DATA

4.1 Calculation of enthalpy and x from horizontal discharge test data

The results from the 4 locations were analyzed using standard James Lip method. Calculated results are shown in Table 1 below.

Table 1. Calculations of enthalpy and dryness fraction from horizontal discharge data

	James Lip	Atm =>	0.98		Pipe X sect	322.8262	<=tests 1-3		
					weir = .4				
wk260	test 1	WHP (bar abs)	Lip (bar abs)	Weir (mm)	Rect Weir	Y	h	mass t/h	x
1 % (kg) =>	7.78				w= .4m				
	1	10.98	3.33	190	198.77	0.19	1131.38	290.75	0.176
	2	11.28	3.08	180	183.28	0.19	1135.16	268.76	0.175
	3	11.98	1.88	110	87.56	0.15	1300.90	143.88	0.253
wk253	test 2								
1 % (kg) =>	5.94								
	1	11.38	2.88	195	206.66	0.23	1024.53	282.73	0.119
	2	11.98	2.68	180	183.28	0.22	1054.57	255.40	0.129
	3	13.73	2.28	165	160.86	0.23	1039.98	222.15	0.109
wk258	test 3								
1 % (kg) =>	7.78								
	1	9.18	2.98	200	214.66	0.23	1021.48	293.14	0.136
	2	12.4	2.08	194	205.08	0.31	855.04	254.43	0.025
wk222	test 4				Pipe X sect	178.18	<= (5.93 inch ID)		
1 % (kg) =>	18.09				weir = .3				
	1	7.38	2.03	110	65.67	0.19	1154.74	97.54	0.218
	2	8.88	1.95	98	55.22	0.16	1238.70	86.81	0.245
	3	11.18	1.53	94	51.88	0.19	1132.83	75.95	0.175

Note that the results of test 3 show a low value for overall well enthalpy. It has been discussed that this may be due to measurement difficulties during the horizontal discharge test.

The calculation of enthalpy and dryness fraction from load cell data is complicated by the difficulty in obtaining a form of initial value for weight without detailed knowledge of the weight of the structural components when empty of water flow. Instead, historical or current horizontal discharge data will be used for calibration. For example, the value of dryness fraction from the first data point taken for the horizontal discharge will be set to be the first data point value of dryness fraction for calculation of load cell data. This assumes that the value of dryness fraction calculated from the first dataset in each horizontal discharge calculation is the ‘true’ value, and the measured weight from the load cells at that point will be set to be the actual weight of that percent of water in the pipe. Then calculation of additional points will be based on that chosen dryness fraction.

4.3 Calculating changes in dryness fraction from changes in percentage of water in the pipe

Dryness fraction (x) is defined as the proportion, by weight, of dry steam in a mixture of steam and water (Science Dictionary.2014). A 1% change in water weight in the pipe structure measured by a load cell would be equal to a 1% change in dryness fraction. Changes in dryness fraction can be calculated from the change in weight measured by the load cell at a pipe support as shown:

$$x (init) - (\Delta w / (w1 \times 100)) = x (new)$$

where

$x (init)$ = initial value of x

Δw = change in weight (delta weight) seen after valve change

w1 = weight of a 1% change in water volume in the measured pipe length

$x (new)$ = new value of x

Using this technique, and setting $x (init)$ equal to the initial value of dryness fraction calculated from horizontal discharge data, values of dryness fraction and enthalpy can be calculated from load cell data(Table 2).

Table 2: Calculations of enthalpy and x from load cell data

			Sensor							
			992	993	992	993	992	993	992	993
wk260	test 1	WHP (bar abs)	Delta kg	Delta kg	Delta x	Delta x	x (new)	x (new)	h	h
1 % (kg) =>	7.78									
	1	10.98					0.176	0.176	1131.38	1131.38
	2	11.28	4.86	4.701	0.006247	0.006042	0.170	0.170	1125.35	1125.75
	3	11.98	16.84	24.72	0.021645	0.031774	0.148	0.138	1092.36	1072.65
wk253	test 2									
1 % (kg) =>	5.94									
	1	11.38					0.119		1024.53	
	2	11.98	18.29		0.030791		0.088		973.12	
	3	13.73	10.16		0.017104		0.071		964.97	
wk258	test 3									
1 % (kg) =>	7.78									
	1	9.18					0.136		1021.482	
	2	12.4	68.49		0.088033		0.047		898.99	
wk222	test 4									
1 % (kg) =>	18.09									
	1	7.38					0.218	0.218	1154.74	1154.74
	2	8.88	50.58	-0.742	0.02796	-0.00041	0.190	0.218	1125.92	1183.57
	3	11.18	69.1	61.38	0.038198	0.03393	0.152	0.184	1087.03	1151.38

Results of the load cell data based on this method of calibration are compared to the results from the horizontal discharge tests in the graphs below.

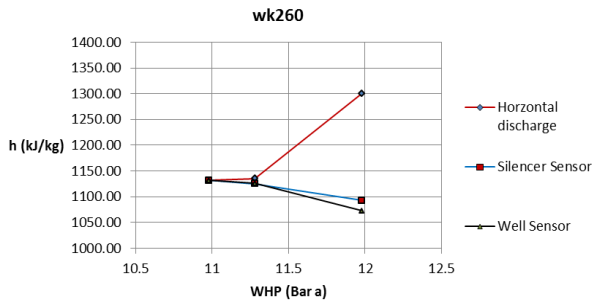


Figure 13: Enthalpy vs WHP. Location 1 (wk260)

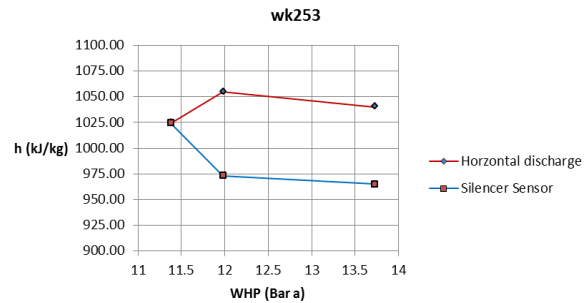


Figure 14: Enthalpy vs WHP. Location 2 (wk253)

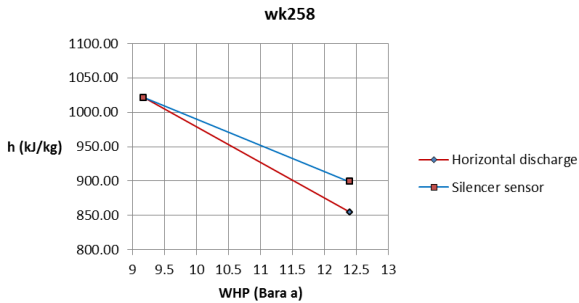


Figure 15: Enthalpy vs WHP. Location 3 (wk258)

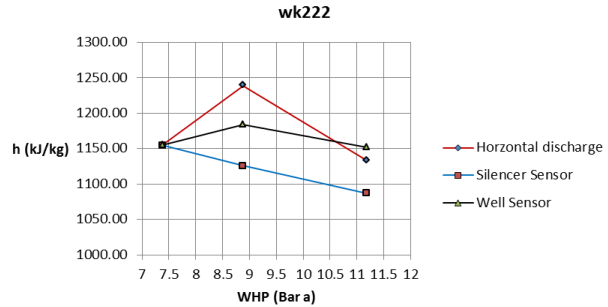


Figure 16: Enthalpy vs WHP. Location 4 (wk222)

4.4 Discussion

In review of the results, the slope of the enthalpy curves for load cell data appears to be a relatively close match to the slope of enthalpy curves from horizontal discharge data. This is interesting, as the change in readings which defines the slope is based on the calculation of dividing the actual measured weight difference between measurements by the theoretical weight of 1% of water. The volume of water used to define this 1% weight is based on the simple static model discussed in section 2.2. Having obtained a relatively close match to slope of the enthalpy curves for both the sensor data and the horizontal discharge data, the difference in readings between the two methods may be mostly related to the choice of start the point for the load cell calculations.

For location 1 (wk260), the first two test points are a good match. However the third shows a major shift when compared to field data.

For location 2 (wk253), the change from test point two to test point three matches the change seen in the horizontal discharge data, but the initial calibration of using the first horizontal discharge point as the starting point for the load cell data may not have been the best point to use for the calibration.

For location 3 (wk258), the results from the horizontal discharge test show low values of enthalpy. As mentioned above, these results are used as the start point for the load cell calculations. No attempt to determine a different start value for load cell calculations has been made.

For location 4 (wk222), the two sensors measured different trends. The sensor near the well appears to match the rising and dropping enthalpy curve also seen in the horizontal discharge data, whereas the second sensor located closer to the silencer shows a more straightforward linear dropping curve. A comparison of both load cell enthalpy curves to the linear trend line of the horizontal discharge data is shown in Figure 18 below.

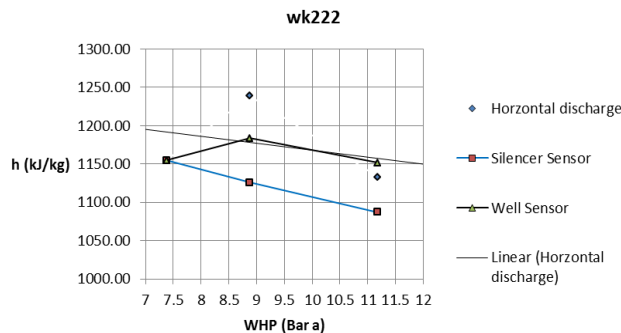


Figure 17: Location 4 (wk222). Load cell results compared to trend line of horizontal discharge data

Viewed in this manner, the result of the sensor near the well is a close match to the linear trend line of the horizontal discharge data. The sensor near the silencer is a close match in slope to the linear trend line and could have an even closer match with a more suitable choice for the initial calibration value of the dryness fraction.

In general the load cell sensor method appears to be able to match trends in horizontal discharge data, with a proper choice of calibration.

5. FURTHER DATA ANALYSIS

5.1 Detection of slug flow

The previous analysis uses load cell data that has been averaged with a specific weighted average. This helps dampen and hide the rapid changes seen by the sensor and allows for easy comparison of the sensor data to the horizontal discharge data. Further flow information, such as details of flow regime, may be able to be determined by analysis of the raw data directly. For example, analysis of the standard deviation of the raw data shows clear evidence of a major change in vibration after certain valve opening changes.

Location 1 and 3 use similar piping configuration. For both tests the load cell data show a major change in vibration when the wells were throttled to minimum flow. These flow rates were chosen because the output showed signs of slug flow, and the wells were therefore not throttled any further. Analysis of the raw data with a running standard deviation, set to one minute intervals, shows a clear pattern. This is shown for location 1 and 3 in Figures 18 and 19.

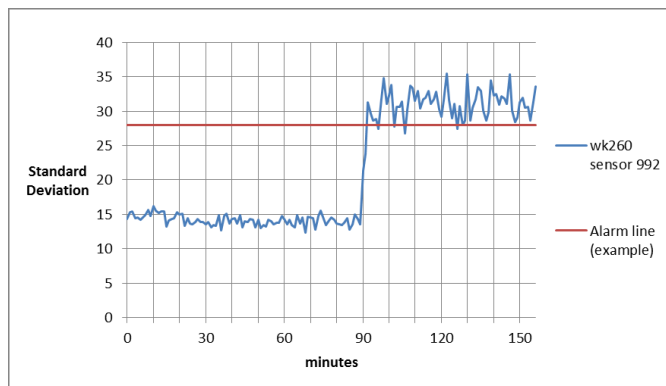


Figure 18: location 1 (wk260) standard deviations

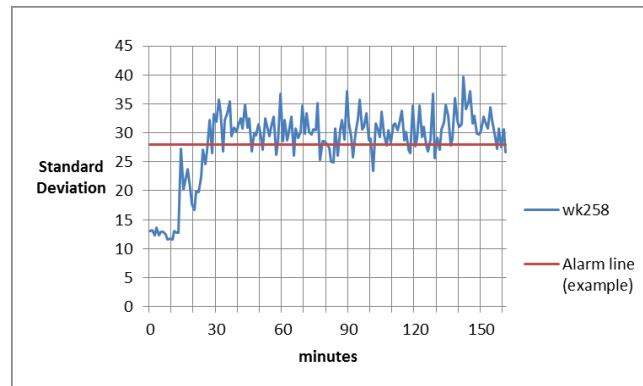


Figure 19: location 3 (wk258) standard deviations

The distinct difference in standard deviation after the valve changes on each well can be used as a means to detect undesirable flows such as slug flow. An ‘alarm level’ as shown in the graphs, could be defined, thereby allowing the sensor to act as a slug flow alarm.

6. CONCLUSION

Load cell sensors were successfully tested at multiple well sites at Wairakei steam fields, New Zealand. Suitable stands were built and modified as necessary to allow for the tests to proceed, and full datasets were taken from one and sometimes two load cell sensors at various field trial sites. Simulations of piping structures were completed and appeared to show that complex pipe stress phenomenon may not be a major contributor to load cell weight readings. Initial set values for the sensor may best be taken from historical information or standard well output tests, and from such values the sensor may be able to correctly track the trends of change taking place in the fluid flow. The four field trials all displayed different phenomenon, allowing for much knowledge to be gained on load cell sensor performance. The load cell sensor was able to measure results of every change done to the wells, with clear tracking of valve changes, and in at least one case was able to measure changes the well had undergone on its own. The sensor accuracy and data rate allow for determination of rapid transitions in value, from laminar flow to turbulent flow, and could be defined as a detector or alarm of such events. The measurement technique may also be used to predict the buildup of mineral scaling in two-phase or single phase pipelines, by tracking the increase in weight of the pipe during use. Full datasets were taken from four different field trial sites and will be used for further analysis. More information, such-as mass flow rate and output enthalpy, may be determined from the datasets obtained.

REFERENCES

Science Dictionary. (2014). Retrieved from <http://thesciencedictionary.org/dryness-fraction/>

Helbig, S., and Zarrouk, S. J.: Measuring two- phase flow in geothermal pipelines using sharp edge orifice plates. *Geothermics*, 44, 52-64. (2012).

Grant, M., and Bixley, P.: *Geothermal Reservoir Engineering*, second edition. Elsevier Inc. (2011).

Arnold, W. A.: *Geothermal Engineering : fundamentals and applications* New York : Springer. (2013).

Sisler, Zarrouk, Urgel, Lim, Adams, and Martin

Outinen, J., and Mäkeläinen, P.: Mechanical properties of structural steel at elevated temperatures and after cooling down. *Fire and Materials*, 28(2), 237-251. (2004).